NASA TECHNICAL NOTE

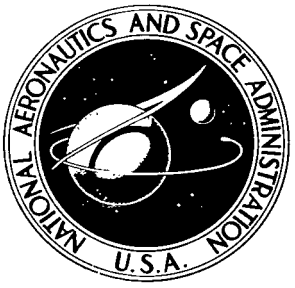

NASA TN D-6315

EXPERIMENTS ON THE STABILITY OF WATER-LUBRICATED THREE-LOBE HYDRODYNAMIC JOURNAL BEARINGS AT ZERO LOAD

by Fredrick T. Schuller

Lewis Research Center
Cleveland, Ohio 44135

NATIONAL AERONAUTICS AND SPACE ADMINISTRATION • WASHINGTON, D. C. • APRIL 1971

1. Report No.	2. Government Accession No.	3. Recipient's Catalog No.
NASA TN D-6315		

4. Title and Subtitle	5. Report Date
EXPERIMENTS ON THE STABILITY OF WATER-LUBRICATED THREE-LOBE HYDRODYNAMIC JOURNAL BEARINGS AT ZERO LOAD	April 1971
	6. Performing Organization Code

7. Author(s)	8. Performing Organization Report No.
Fredrick T. Schuller	E-6050
	10. Work Unit No. 129-03

9. Performing Organization Name and Address	11. Contract or Grant No.
Lewis Research Center National Aeronautics and Space Administration Cleveland, Ohio 44135	
	13. Type of Report and Period Covered
12. Sponsoring Agency Name and Address	Technical Note
National Aeronautics and Space Administration Washington, D.C. 20546	14. Sponsoring Agency Code

15. Supplementary Notes

16. Abstract

Hydrodynamic journal bearing stability tests were conducted with three-lobe bearings with and without axial grooves. The bearings had a 3.8-cm (1.5-in.) diameter and length and were tested in water at 300 K (80° F) at speeds to 7000 rpm with zero load. Whirl threshold speed decreases with increasing clearance at a much faster rate in ungrooved than in grooved three-lobe bearings. Tests were conducted with symmetric three-lobe bearings. Results are compared with previous tests of asymmetric lobed bearings. Maximum stability and least sensitivity to clearance are obtained with a three-lobe bearing when the lobes are tilted so that the minimum film thickness occurs at about the trailing edges of the lobes.

17. Key Words (Suggested by Author(s))
Three-lobe bearings
Bearing stability
Water bearings
Bearing fractional frequency whirl
Inexpensive three-lobe bearing fabrication technique
Grooved and ungrooved three-lobe bearings

18. Distribution Statement
Unclassified - unlimited

19. Security Classif. (of this report)	20. Security Classif. (of this page)	21. No. of Pages	22. Price*
Unclassified	Unclassified	24	$3.00

*For sale by the National Technical Information Service, Springfield, Virginia 22151

EXPERIMENTS ON THE STABILITY OF WATER-LUBRICATED THREE-LOBE HYDRODYNAMIC JOURNAL BEARINGS AT ZERO LOAD

by Fredrick T. Schuller

Lewis Research Center

SUMMARY

Stability tests were conducted with 3.8-centimeter- (1.5-in.-) diameter, 3.8-centimeter- (1.5-in.-) long, three-lobe hydrodynamic journal bearings in water at 300 K (80° F) at speeds to 7000 rpm with zero load. The lobes were generated by distortion of the bearing wall with shims at the bearing back. Centrally lobed bearings with and without axial grooves were tested. While lobed bearings with grooves had fair stability over a range of clearances from 0.009 to 0.052 millimeter (350 to 2050 μin.), those without grooves were unstable at minimum operating speed (70 rpm) at clearances above 0.018 millimeter (700 μin.). The stability of a three-lobe bearing is a strong function of lobe height. Comparison of the results of centrally lobed bearings with previous tests of asymmetric lobed bearings indicates that maximum stability is achieved when the lobes are tilted so that the points of minimum film thickness occur near the trailing edges. This agrees well with theory, and results in a bearing stability that is least sensitive to clearance. For centrally lobed bearings maximum stability was attained at a lobe height of approximately 0.025 millimeter (1000 μin.) over a clearance range of 0.015 to 0.052 millimeter (600 to 2050 μin.).

INTRODUCTION

The ability of a journal bearing to inhibit self-excited fractional frequency whirl is of prime importance for successful operation of rotating machinery at conditions of high speed and low loads with a low-viscosity fluid, such as water, as the lubricant. In this type of whirl, the journal center orbits the bearing center at an angular velocity about one-half that of the journal around its own center. Such whirling can fail a bearing. It is desirable, therefore, to select a bearing geometry that has a high degree of stability.

Tilting-pad bearings are exceptionally stable but are complex since they are composed of several parts and may be subject to pivot surface damage (ref. 1). Fixed-geometry bearings do not have the disadvantage of complexity, but they are not as stable as the tilting-pad bearing. A fixed-geometry bearing that showed good stability properties is the herringbone-groove bearing (refs. 2 to 4). Another fixed-geometry bearing that has shown promise is the lobed bearing (ref. 5), which has a marked similarity to the tilting-pad bearing except that its pads (lobes) are fixed in one position.

Experimental stability data on two designs of three-lobe bearings are reported in reference 6. The sectors were tilted so that the minimum film thickness occurred at a point 60 percent of the arc length of the sector from the leading edge of the lobe arc in one design (fig. 1(a)) and at the trailing edge of the lobe arc in the other design (fig. 1(b)). The manner in which the lobes are tilted can be expressed in simpler terms by designating the bearing in which the point of minimum film thickness at zero eccentricity occurs at the trailing edge of its arc length as a lobed bearing with an offset factor of 1.0. A symmetric or centrally lobed bearing would, therefore, have an offset factor of 0.5.

In the investigation reported herein, three-lobe bearings with an offset factor of 0.5 (centrally lobed) were tested. Normally, lobed bearings are fabricated by internal off-center grinding of each lobe. However, for this study, the lobes were generated by the insertion of shims between the bearing housing inside diameter and the outside diameter of a plain cylindrical bearing (fig. 2). At assembly, by means of differential expansion techniques, each shim forces the bearing wall inward in its immediate vicinity, resulting in lobes on the bearing inside diameter.

The objectives of this study were (1) to observe the effect of lobe height on stability of a three-lobe bearing; (2) to compare the stability of a three-lobe bearing with and without axial grooves; (3) to compare experimental stability data for three-lobe bearings with analytical predictions; (4) to generate design curves to facilitate the design of optimum-geometry three-lobe bearings; and (5) to compare the stability of centrally lobed bearings (offset factor of 0.5) with bearings having offset factors of 0.6 and 1.0.

A bearing with three lobes was selected for this study so that the stability results could be compared directly with those of previously tested three-sector bearings of the same size reported in reference 6 and because analyses are available for the three-lobe bearing geometry, in references 5 and 7. The test bearings had a nominal 3.8-centimeter (1.5-in.) diameter and were 3.8 centimeters (1.5 in.) long. They were submerged in water at an average temperature of 300 K (80° F) and were operated hydrodynamically at journal speeds to 7000 rpm.

SYMBOLS

a	preload (ellipticity), mm; in.
C	bearing radial clearance, $R_{PC} - R$, mm; in.
C_o	bearing radial clearance at zero preload, $R_P - R$, mm; in.
D	journal diameter, cm; in.
g	gravitational constant, m/sec^2; $in./sec^2$
H_L	lobe height, mm; in.
k	film thickness ratio, $1 + (H_L/C)$
L	bearing length, cm; in.
M	rotor mass per bearing, W_r/g, kg; $(lb)(sec^2)/in.$
$\overline{M}$	dimensionless mass parameter, $MP_aC^5/2\mu^2LR^5$
$\overline{M}_o$	dimensionless rotor mass parameter, $C_oMN_S/\mu DL(R/C_o)^2$ (ref. 5)
N_S	journal speed, rps
N_W	journal fractional-frequency-whirl onset speed at zero load, rpm
P_a	atmospheric pressure, N/m^2 abs; psia
R	journal radius, cm; in.
Re	Reynolds number, $2\pi\zeta RN_SC_o/\mu$
R_P	radius of sector, cm; in.
R_{PC}	radius of pitch circle, cm; in.
W_r	total weight of test vessel, N; lb
α	offset factor, θ/β
β	sector arc length, deg
Γ	dimensionless speed parameter, $6\mu\omega R^2/P_aC^2$
δ	preload coefficient, $a/(R_P - R)$
ζ	mass density, kg/m^3; $(lb)(sec^2)/in.^4$
θ	arc length from leading edge of sector to the line along which the lobe is preloaded radially
μ	lubricant dynamic viscosity, $(N)(sec)/m^2$; $(lb)(sec)/in.^2$
ω	journal angular velocity, rad/sec

APPARATUS

Test Bearings

Three-lobed bearings with and without axial grooves separating the lobes were evaluated. The bearings were lobed by the use of shims in a unique manner as presented in a recent patent disclosure (ref. 8) and shown in figure 2. The procedure for fabricating a shimmed, lobed bearing is as follows:

(1) A plain cylindrical bearing is assembled into a housing (fig. 2), with a light interference fit by cooling the bearing or heating the housing and depositing the bearing into the housing.

(2) The bearing is machined in place to a predetermined round inside diameter, and an identification mark is scribed on the top surface of the bearing and housing.

(3) The bearing is removed from its housing by cooling the assembly. (If the expansion coefficient of the housing is greater than that of the bearing, heat can be used for the disassembly operation.)

(4) Equally spaced metal shims approximately 3 millimeters (1/8 in.) wide are placed axially around the inside diameter of the housing and are tack-welded or taped to the top and bottom of the bearing housing to prevent their dislocation. The thickness of the shims depends upon the lobe height desired.

(5) The bearing is assembled into the shimmed housing by cooling the bearing or heating the housing and placing the bearing into the housing with the identification marks on the bearing and housing lined up with each other.

(6) When the bearing and housing have reached thermal equilibrium, a profile trace of the inside diameter will indicate accurately what size lobing has been attained. The amount of lobing will depend upon the thickness of the shims and the physical properties of the bearing housing, shim stock, and bearing materials used.

A typical bearing assembly used in this report had the following dimensions:

Housing (stainless steel)	
Outside diameter, cm (in.)	10.79 (4.250)
Inside diameter, cm (in.)	5.0411 (1.9847)
Bearing (bronze)	
Outside diameter, cm (in.)	5.0419 (1.9850)
Inside diameter, cm (in.)	3.8199 (1.5039)
Interference fit between bearing and housing, mm (μin.)	0.008 (300)
Shim (steel)	
Width, mm (in.)	3 (1/8)
Thickness, mm (in.)	0.025 (0.0010)
Resultant lobe height of bearing, mm (in.)	0.025 (0.0010)

A typical circumferential profile trace of the inside surface of the shimmed test bearing is shown in figure 3. The height of the lobes H_L was determined from similar traces for each of the test bearings used in this study.

Figure 4 shows the parameters which define the centrally lobed bearing geometry employed in this investigation. The angle θ is defined as the arc length from the leading edge of a sector to the point of minimum film thickness at zero eccentricity. In this case $\theta = 0.5\,\beta$. The offset factor $\alpha = \frac{\theta}{\beta}$ for the centrally lobed bearing is, therefore, 0.5. The preload coefficient δ is equal to the preload a divided by the difference between the radius of the lobe, which in conventionally lobed bearings is machined in, and the radius of the journal $\delta = a/(R_P - R)$. However, in this case the lobe was generated by distortion of the bearing wall, so the radius of the lobe R_P had to be calculated from the lobe height values H_L obtained from the profile traces (fig. 3) of each bearing tested.

The difference in contour between the lobes of a conventionally machined lobe bearing and those of a bearing formed by shimming will be discussed in more detail in the section Comparison of Theoretical and Experimental Stability Data for Three-Lobe Three-Axial-Groove Bearings.

The assembled bearings in all cases had a nominal 3.8-centimeter (1.5-in.) length and diameter. The inside surface of the bearing and the journal outside diameter were machined to a 0.1- to 0.2-micrometer (4- to 8-μin.) rms finish. The journals were made of 17-4 PH stainless steel and the lobed bearings of bronze.

Bearing Test Apparatus

The test vessel and associated parts are shown in figure 5. The shaft is positioned vertically so that gravity forces do not load the bearing. The test vessel, which also serves as the test bearing housing, floats between the upper and lower gas bearings. Bearing torque can be measured, if desired, by a force transducer attached to the floating test vessel.

Movement of the test vessel during a test is measured by orthogonally mounted capacitance probes outside the test vessel. The output of the probes is connected to an X, Y-display on an oscilloscope, where this motion can be observed. The orbital frequency of the test vessel motion was measured by a frequency counter. A more detailed description of the test apparatus and instrumentation is given in reference 2.

PROCEDURE

Details of the test procedure are given in reference 2. The bearings were run at zero load throughout the entire test. The onset of whirl was noted by observing the bearing housing motion on the oscilloscope screen (ref. 2). The shaft speed was recorded at this time. Damage to the test bearings due to fractional-frequency whirl was prevented by reducing the speed immediately after photographing the whirl pattern on the oscilloscope screen.

In these experiments, the motion of the bearing with its massive housing was monitored. Thus, the journal axis was fixed while the bearing axis whirled. The validity of the stability data obtained in this manner was established in reference 2, where excellent correlation was obtained between theoretical and experimental data for a three-axial-groove bearing run in water with a plain journal.

RESULTS AND DISCUSSION

General

Experimental results obtained with ten bearings having different lobe heights are shown in tables I to IV. Test results for three-lobe bearings with three axial grooves are shown in table I, and those with no axial grooves are shown in table IV. Table II lists the results for a three-axial-groove bearing with no lobing, and table III the results for a plain bearing with no grooves and no lobing. Journals of different diameters were used to obtain the different clearances shown for any particular bearing tested. A total of 39 bearing stability tests was conducted at values of radial clearances C ranging from 0.009 to 0.052 millimeter (350 to 2050 μin.), and lobe heights ranging from 0 to 0.102 millimeter (0 to 4000 μin.).

The bearings were submerged in water at an average temperature of 300 K (80° F) and run hydrodynamically. Maximum speed attained without whirl was 7000 rpm.

Effect of Lobe Height on Stability

The experimental results obtained with three-lobe bearings with axial grooves are shown in figure 6(a). In the area labeled stable operation, to the left of the experimental curves, the bearings ran stably at zero load; to the right of the curves, fractional frequency whirl occurred. The experimental curves represent the stability limits of the bearings tested and indicate the zero load threshold of stability. The dimensionless

mass parameter $\overline{M}$ and the dimensionless speed parameter Γ were obtained from the theoretical stability analysis in reference 2. Figure 6(a) shows the stability limits of a three-lobe, three-axial-groove bearing at five different lobe heights. As the lobe height was increased from 0 to 0.25 millimeter (0 to 1000 μin.), the stability increased. (The bearing having a lobe height of zero is actually a plain (unlobed) bearing with three axial grooves.) As the lobe height was further increased from 0.025 to 0.066 millimeter (1000 to 2600 μin.), the stability decreased. Maximum stability occurred at a lobe height of 0.025 millimeter (1000 μin.).

Figure 6(b) shows the stability limits of three-lobe bearings with no axial grooves at five different lobe heights. Maximum stability occurred at a lobe height of 0.025 millimeter (1000 μin.) for the limited data recorded. (There were no data obtained at lobe heights below 0.025 millimeter (1000 μin.), except for the zero lobe height value.) An increase in lobe height above 0.025 millimeter (1000 μin.) caused a decrease in stability.

Range of Stability of a Three-Lobe Bearing With and Without Axial Grooves

It is interesting to note that stable operation at a clearance value above 0.018 millimeter (700 μin.) was impossible to attain with the three-lobe bearing without the three axial grooves (table IV). It appears that at the tighter clearances, 0.013 to 0.018 millimeter (500 to 700 μin.), the lobes of the bearing without grooves are effective in keeping the bearing stable. However, as the clearance is increased above 0.013 millimeter (700 μin.), the lobes lose their effectiveness and the bearing no longer acts as a bearing of three distinct sectors but as a plain bearing with a uniformly distorted contour. An attempt was made to run a plain cylindrical bearing with no grooves and zero lobe height, representing a minimum condition of lobe height for the bearings without grooves. This bearing ran stably at a clearance of 0.009 millimeter (350 μin.) to a speed of 6200 rpm but was completely unstable at a clearance of 0.018 millimeter (700 μin.) (table III). Since an unloaded plain journal bearing will whirl at all speeds and clearances, the one stable point at 0.009 millimeter (350 μin.) was probably due to a slight misalinement of the bearing with the journal. This would tend to preload the bearing and give it some stability (ref. 9). At higher clearances, above 0.009 millimeter (350 μin.), the preload was too small to preload the bearing effectively and keep it running stably.

From the results of the present investigation it is apparent that a three-lobe bearing with three axial grooves is stable over a larger range of clearances than one without grooves when operating hydrodynamically while immersed in a low-viscosity lubricant such as water.

Comparison of Theoretical and Experimental Stability Data for Three-Lobe Three-Axial-Groove Bearings

The solid curves shown in figure 7 are from reference 5 and show the theoretical stability threshold of three-lobe bearings that are centrally lobed. Since the Reynolds number of the experimental points reported herein fell within the range of 0 to 2000, both curves have been included. The experimental data were plotted using the parameters of reference 5 and show fair agreement with the theoretical values for the centrally lobed bearing (offset factor $\alpha = 0.5$). Theory predicts a larger range of stable operation than was observed experimentally.

Conventionally the lobe radius is machined in the bearings, and this radius is then measured. Using shims to obtain the lobes, as was done here, results in a lobe contour that is not exactly a true circular arc. Therefore, a radius which approximates the curvature of the lobes had to be calculated from the lobe height readings. Figure 8 shows the difference in lobe contour between a lobe that has been machined in and a lobe that has been generated by a shim. The contour of the shimmed lobe is shown as a solid curve and was traced from a profile trace of one of the test bearings. The dashed curve illustrates what the contour would look like if it were machined in and generated from the 120° arc to the right of the curves. Both lobes have the same height, 0.025 millimeter (1000 μin.). Although there is a slight difference in contour, applying circular-arc theory to the shimmed bearings seems valid in light of the following argument. Figure 9 shows the theoretical curves of reference 5, repeated from figure 7, along with two experimental curves. The short-dash curve represents a smooth curve that was drawn through the collective data for a series of bearings with machined lobes having an offset factor of 0.6 (ref. 6). The long-dash curve represents a smooth curve that was drawn through the experimental data shown in figure 7 for lobed bearings with an offset factor of 0.5 which had lobes generated by shims. It was shown in reference 6 that increased stability can be obtained by tilting each bearing sector towards its trailing edge; therefore, a bearing with an offset factor of 0.6 will be more stable than one with an offset factor of 0.5. It appears, then, that the theoretical curves of figure 9 which are for lobed bearings of 0.5 offset factor should be more accurately located near the experimental curve of the 0.5 offset factor bearings. This would place the experimental curve for the lobed bearings with a 0.6 offset factor above the theoretical curves of offset factor 0.5. From the results of at least these two experimental studies it appears that any discrepancy between theoretical and experimental results is due to some factor that was not considered in the theoretical analysis. The effect that differences in lobe contour might have on stability could only be determined if the results of these shimmed lobe bearing tests were compared with those of machined-in lobe bearings of equal offset factor and dimensions.

The calculated lobe radius R_P is the same radius that would be used to machine a lobe of the same height as the shimmed lobe. A sample calculation follows to show how the measured lobe height of the shimmed bearings was used to obtain R_P. Figure 10 is an illustration of the pitch circle of a three-lobe bearing and one of the centrally lobed sectors. The pitch circle is defined as a circle that touches each lobe at its minimum film thickness location (the midpoint of each lobe arc for centrally lobed bearings). A triangle based on the relation between the pitch circle and lobe radii is constructed as shown. From the law of cosines

$$(R_{PC} + a)^2 = (R_{PC} + H_L)^2 + (a)^2 - 2\,(R_{PC} + H_L)\,(a)\,(\cos 120^\circ) \qquad (1)$$

In this example the lobe height H_L was measured to be 0.025 millimeter (1000 μin.) and the pitch circle radius was measured to be 1.909 centimeter (0.7514 in.). Substituting these known values in equation (1) results in a value of 0.050 millimeter (2000 μin.) for the preload a. The lobe radius R_P is the sum of the pitch circle radius R_{PC} and the preload a, or in this case 1.909 + 0.0050 = 1.914 centimeters (0.7514 + 0.0020 = 0.7534 in.). The preload coefficient is then obtained from $\delta = a/(R_P - R)$ and would be the same for a machined lobe of equal height.

Design Curves

The data were replotted in slightly different form in order to facilitate the design of optimum-geometry bearings. Whirl onset speed is plotted against radial clearance in figure 11 for the four different values of lobe height H_L for the three-lobe axially grooved bearings. The values of film thickness ratio, $k = 1 + (H_L/C)$, and preload coefficient, $\delta = a/(R_P - R)$(table I), are given for each data point. Vertical dashed lines intersect the experimental curves at four arbitrary clearance values. The curves in figure 12 were obtained by cross-plotting the data in figure 11 at the four different values of clearance, using the whirl speed N_W and the film thickness ratio k and preload coefficient δ as the coordinates. Simple straight-line interpolation was used for the cross plot. Figure 12 shows that there is an optimum value of k and δ at any given C and that this optimum is a function of C. It also shows that stability becomes more sensitive to k as C increases, although this is not readily apparent because of the nonuniform scale used in plotting k in this figure.

Figure 13 is essentially a repetition of figure 12 except that it was plotted by using the dimensionless speed parameter Γ instead of whirl onset speed as the ordinate. It is included because it is more useful as a design parameter than the curves of figure 12.

Preload coefficient is a more universal term used in lobed bearing design than is film thickness ratio. Lobe height is only used in this report because it was the dimension that was measured and from this measured dimension the radius of the sector R_p was calculated to arrive at the preload coefficient $\delta = a/(R_p - R)$. For this reason both preload coefficient δ and film thickness ratio k appear as coordinates in figures 12 and 13.

Figures 12 and 13 show that the preload coefficient, at the points of optimum locus, increases from about 0.54 to 0.78 and the film thickness ratio from 1.57 to 2.78 as the clearance is reduced from 0.046 to 0.015 millimeter (1800 to 600 μin.).

Three-Lobe Bearing Geometry of Maximum Stability

The offset factor α of a lobed bearing is defined as the ratio of the arc length from the leading edge of the sector to the point of minimum film thickness at zero eccentricity θ to the arc length of the sector β (fig. 4). Figure 14 shows a comparison of the stability of three-lobe bearings with various offset factors. Whirl speed is plotted against radial clearance for bearings of three different offset factors, 0.5, 0.6, and 1.0. The points for the three-lobe bearing with an offset factor of 0.5 correspond to the points of maximum stability (optimum locus curve) obtained from figure 12. The points for the bearings with an offset factor of 0.6 and 1.0 were obtained in a similar manner from the experimental data reported in reference 6. As the offset factor is increased from 0.5 to 1.0 in figure 14, the curves shift to the upper right at a shallower slope, which indicates an increase in stability and less sensitivity to clearance.

An analytical study of the three-lobe bearing was reported in reference 7, which showed that a maximum in stability for a three-lobe bearing with an $L/D = 1$ occurred at an offset factor of about 0.9. This agrees with the experimental data of figure 14, which shows an offset factor of 1.0 to be more stable than an offset factor of 0.5 or 0.6.

SUMMARY OF RESULTS

A total of 39 stability tests was performed on two types of centrally lobed three-lobe bearings. One type had an axial groove separating each lobe arc and the other type had no grooves. Bearings of each type, having a variety of lobe heights, were run at a number of different radial clearances. The clearances varied from 0.009 to 0.052 millimeter (350 to 2050 μin.), and the lobe heights from 0 to 0.102 millimeter (0 to 4000 μin.).

The bearings were run hydrodynamically in water at an average temperature of 300 K (80° F) at speeds to 7000 rpm. The test bearings had a diameter of 3.8 centimeters (1.5 in.) and a length-diameter ratio of 1.

The lobes on the test bearings were generated by means of shims inserted at three equidistant lines between the bearing back and housing rather than by conventional machining techniques. The following results were obtained:

1. Maximum stability of a three-lobe centrally lobed bearing with axial grooves occurred at a lobe height of 0.025 millimeter (1000 μin.) over a clearance range of 0.015 to 0.052 millimeter (600 to 2050 μin.).

2. Stable operation of a three-lobe bearing without axial grooves was impossible to attain at clearances above 0.018 millimeter (700 μin.) over a range of lobe heights from 0.025 to 0.102 millimeter (1000 to 4000 μin.).

3. Experiments indicate a smaller range of stable operation for three-lobe centrally lobed bearings than predicted by theory.

4. An optimum value of preload coefficient exists at any given clearance, and this optimum is a function of clearance.

5. Experimental data indicate that, as the offset factor (angle from leading edge to the minimum-film-thickness point at zero eccentricity/lobe angle) of a three-lobe bearing is increased from 0.5 to 1.0, the stability increases and becomes less sensitive to clearance. This agrees well with theory, which predicts maximum stability at an offset factor of 0.9.

Lewis Research Center,
National Aeronautics and Space Administration,
Cleveland, Ohio, January 28, 1971,
129-03.

REFERENCES

1. Schuller, Fredrick T.; Anderson, William J.; and Nemeth, Zolton N.: Operation of Hydrodynamic Journal Bearings in Sodium at Temperatures to 800° F and Speeds to 12,000 rpm. NASA TN D-3928, 1967.

2. Schuller, Fredrick T.; Fleming, David P.; and Anderson, William J.: Experiments on the Stability of Water Lubricated Herringbone-Groove Journal Bearings. I - Theoretical Considerations and Clearance Effects. NASA TN D-4883, 1968.

3. Malanoski, S. B.: Experiments on an Ultrastable Gas Journal Bearing. J. Lubr. Tech., vol. 89, no. 4, Oct. 1967, pp. 433-438.

4. Vohr, J. H.; Chow, C. Y.: Characteristics of Herringbone-Grooved, Gas-Lubricated Journal Bearings. J. Basic Eng., vol. 87, no. 3, Sept. 1965, pp. 568-578.

5. Lund, J. W.: Rotor-Bearing Dynamics Design Technology. Part VII: The Three Lobe Bearing and Floating Ring Bearing. Rep. MTI-67TR47, Mechanical Technology, Inc. (AFAPL-TR-65-45, pt. 7, DDC No. AD-829895), Feb. 1968.

6. Schuller, Fredrick T.; and Anderson, William J.: Experiments on the Stability of Water-Lubricated Three-Sector Hydrodynamic Journal Bearings at Zero Load. NASA TN D-5752, 1970.

7. Falkenhagen, George L.; and Gunter, Edgar J., Jr.: Non-Linear Transient Analysis of a Rigid Rotor Supported by Non-Circular Bearings. Rep. ME-4040-102-70U, University of Virginia, June 1970.

8. Schuller, Fredrick T.: Lobing Technique for a Multilobed Bearing. NASA Case No. 10, 296-1, Disclosed Aug. 3, 1967.

9. Boeker, G. G.; and Sternlicht, B.: Investigation of Translatory Fluid Whirl in Vertical Machines. Trans. ASME, vol. 78, no. 1, Jan. 1956, pp. 13-19.

TABLE I. - TEST RESULTS FOR THREE-LOBE BEARINGS WITH THREE AXIAL GROOVES

Bearing	Lobe height, H_L		Preload (ellipticity), a		Minimum radial clearance, $C = R_{PC} - R$		Radial clearance before preload, $C_o = R_P - R$		Fractional frequency whirl onset speed at zero load, N_W, rpm	Film thickness ratio, $k = 1 + \frac{H_L}{C}$	Preload coefficient, $\delta = \frac{a}{R_P - R}$
	mm	μin.	mm	μin.	mm	μin.	mm	μin.			
8M	0.015	600	0.030	1200	0.014	550	0.044	1750	5000	2.09	0.685
					.020	800	.051	2000	670	1.75	.600
					.025	1000	.056	2200	300	1.60	.545
					.039	1550	.070	2750	200	1.39	.438
					.052	2050	.083	3250	90	1.29	.367
8	0.025	1000	0.051	2000	0.015	600	0.066	2600	4900	2.67	0.770
					.024	950	.076	3000	2000	2.06	.680
					.039	1550	.091	3600	500	1.65	.565
					.052	2050	.104	4100	160	1.49	.494
9	0.046	1800	0.091	3600	0.013	500	0.104	4100	5000	4.60	0.878
					.022	850	.114	4500	2200	3.12	.810
					.037	1450	.130	5100	390	2.24	.713
					.050	1950	.142	5600	100	1.92	.648
10	0.066	2600	0.132	5200	0.010	400	0.142	5600	4300	7.50	0.930
					.024	950	.158	6200	1300	3.74	.848
					.037	1450	.170	6700	200	2.79	.782
					.047	1850	.180	7100	130	2.41	.738

TABLE II. - TEST RESULTS FOR A THREE-AXIAL-GROOVE BEARING WITH NO LOBING (BEARING 7P)

[Film thickness ratio, 1.0.]

Radial clearance, C		Fractional frequency whirl onset speed at zero load, N_W, rpm
mm	μin.	
0.009	350	7000
.023	900	500
.033	1300	250
.046	1800	70

TABLE III. - TEST RESULTS FOR A PLAIN BEARING - NO GROOVES, NO LOBING (BEARING 50)

Radial clearance, C		Fractional frequency whirl onset speed at zero load, N_W, rpm
mm	μin.	
0.009	350	6200
.018	700	(a)

[a]Bearing unstable at minimum operating speed (70 rpm).

TABLE IV. - TEST RESULTS FOR THREE-LOBE

BEARINGS WITH NO GROOVES

Bearing	Lobe height, H_L		Minimum radial clearance, $C = R_{PC} - R$		Fractional frequency whirl onset speed at zero load N_W, rpm
	mm	μin.	mm	μin.	
1	0.025	1000	0.013	500	7000
			.018	700	5400
			.023	900	(a)
			.032	1250	(a)
2	0.048	1900	0.013	500	5500
			.018	700	4400
			.023	900	(a)
			.032	1250	(a)
5	0.076	3000	0.013	500	4500
			.018	700	3800
			.023	900	(a)
			.032	1250	(a)
6	0.102	4000	0.011	450	4300
			.016	650	1200
			.025	1000	(a)
			.029	1150	(a)

[a]Bearing unstable at minimum operating speed (70 rpm).

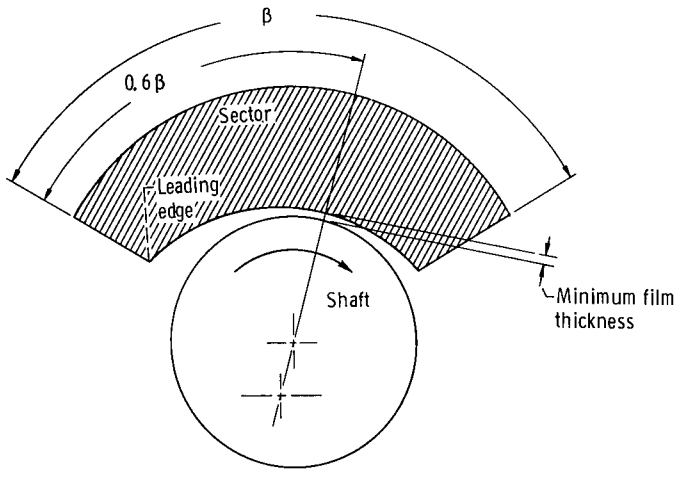

(a) Offset factor, 0.6.

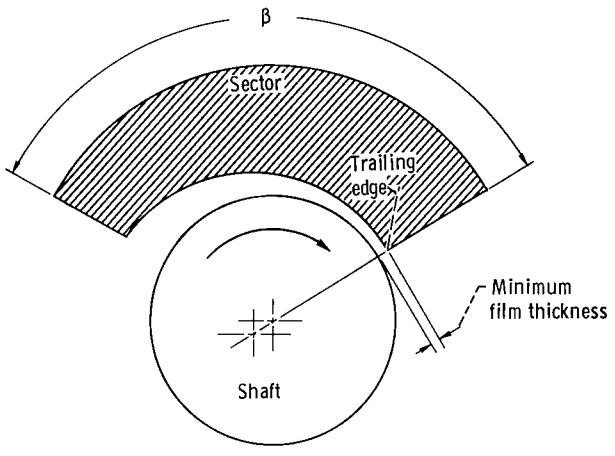

(b) Offset factor, 1.0.

Figure 1. - Sector bearing geometry.

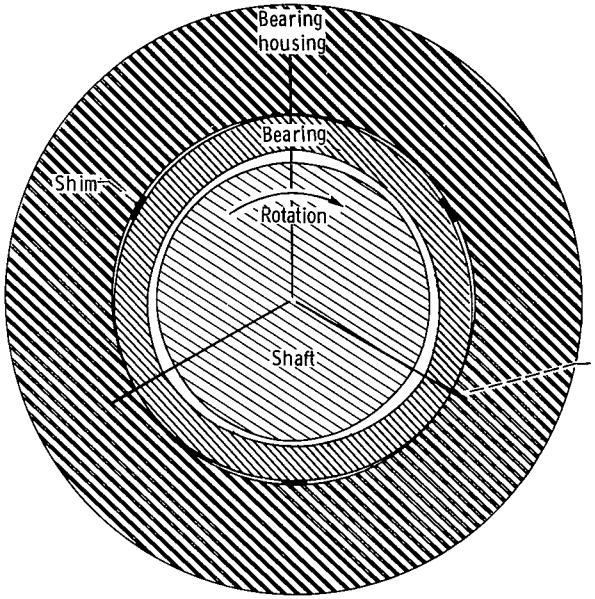

Figure 2. - Three-lobed-bearing assembly.

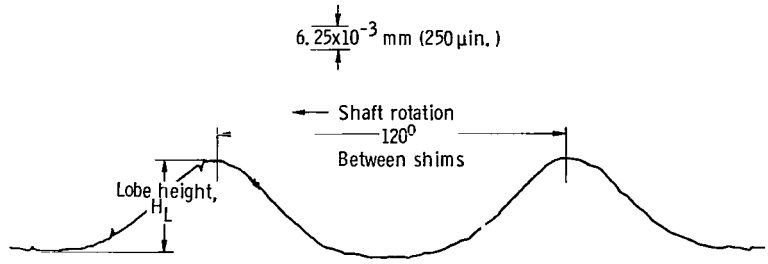

Figure 3. - Typical circumferential profile trace of inside surface of shimmed bearings.

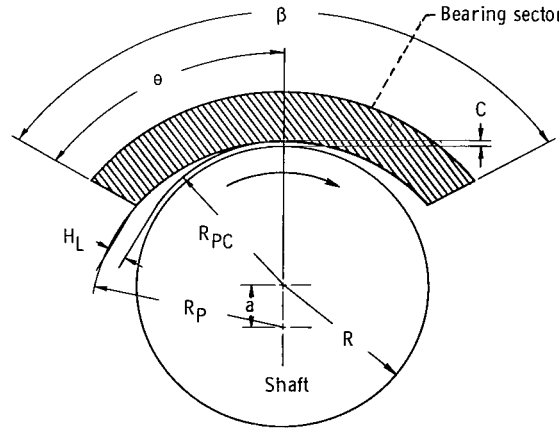

Figure 4. - Bearing geometry for centrally lobed bearing. Offset factor, $\alpha = \theta/\beta$.

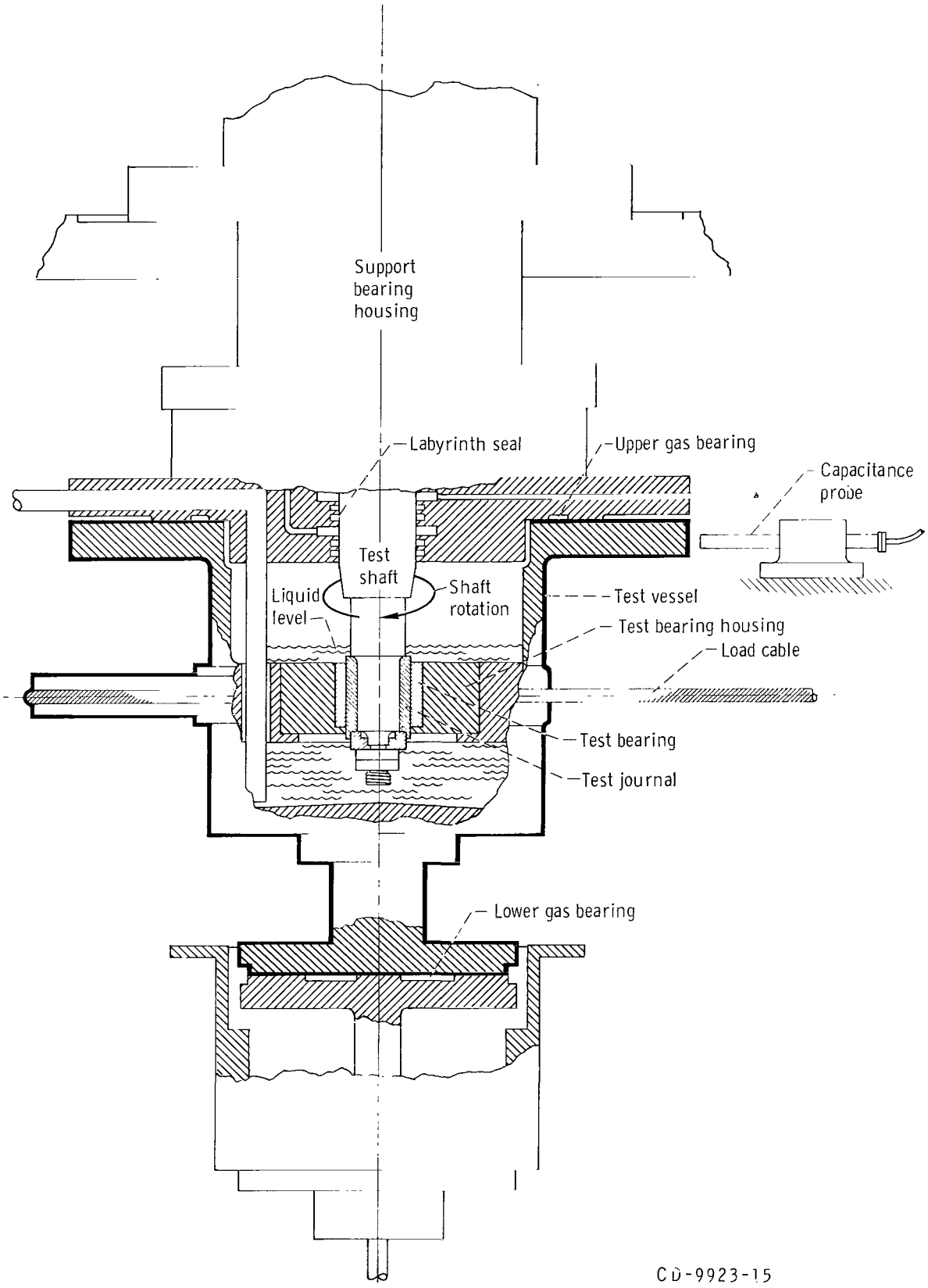

Figure 5. - Bearing test apparatus.

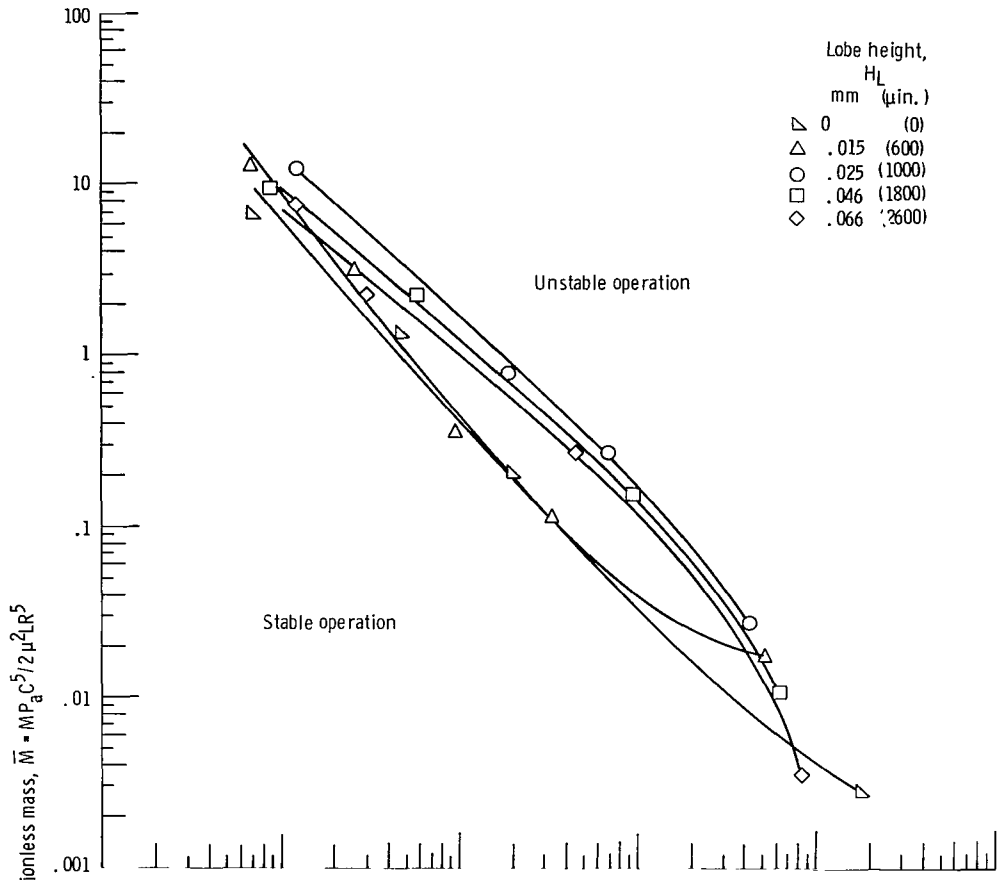

(a) With three axial grooves.

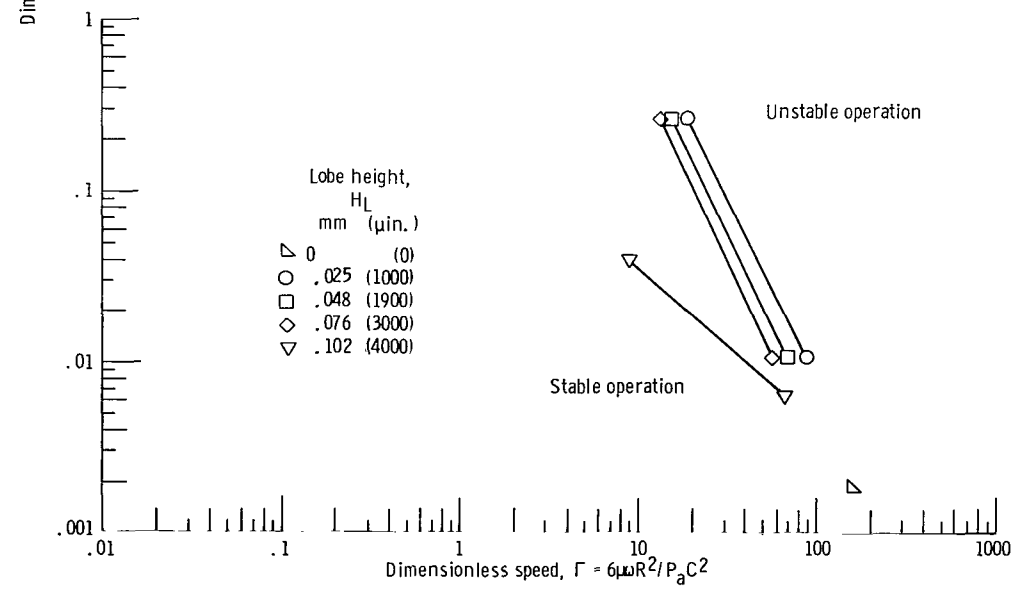

(b) Without grooves.

Figure 6. - Effect of lobe height on stability of centrally lobed three-lobe bearing.

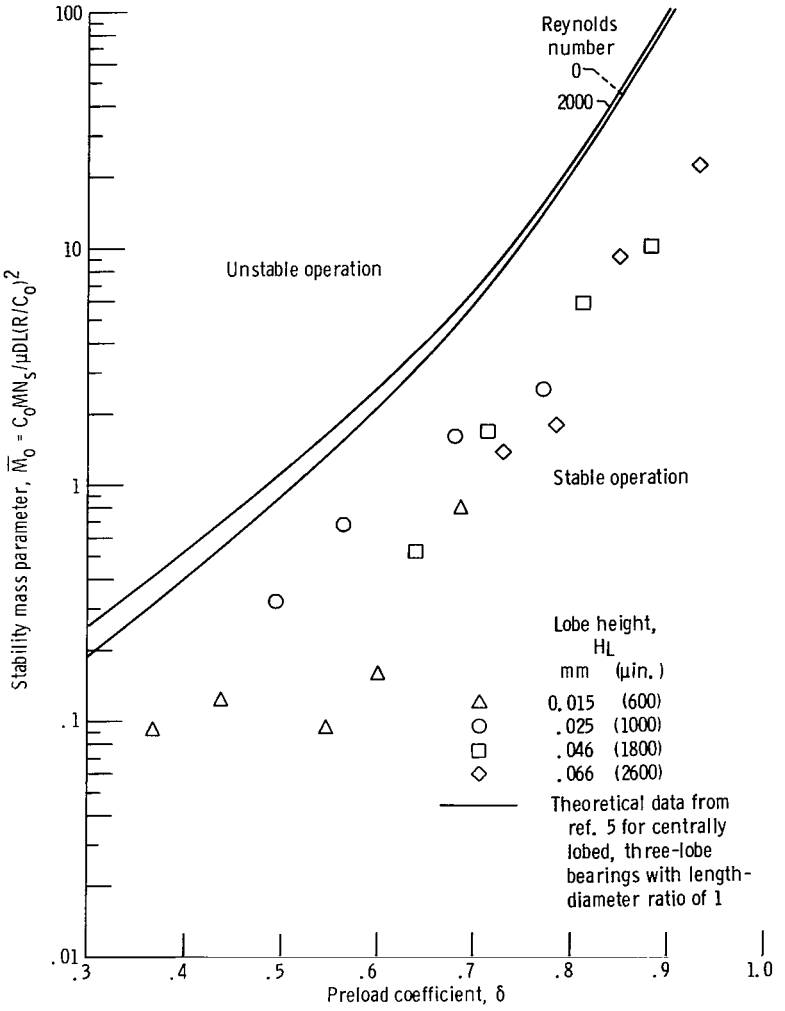

Figure 7. - Comparison of theoretical and experimental data using dimensionless parameters of reference 5.

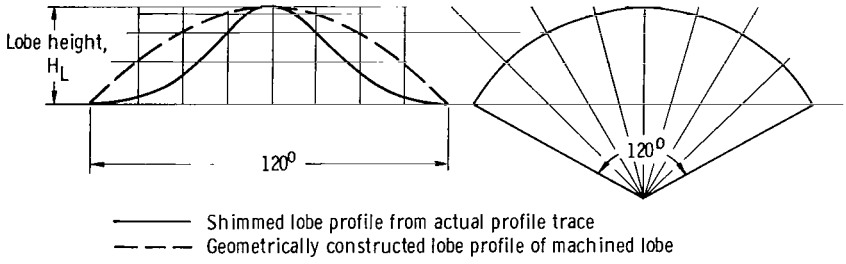

Figure 8. - Comparison of profile of shimmed and machined lobe. Lobe height, 0.025 millimeter (1000 μin.).

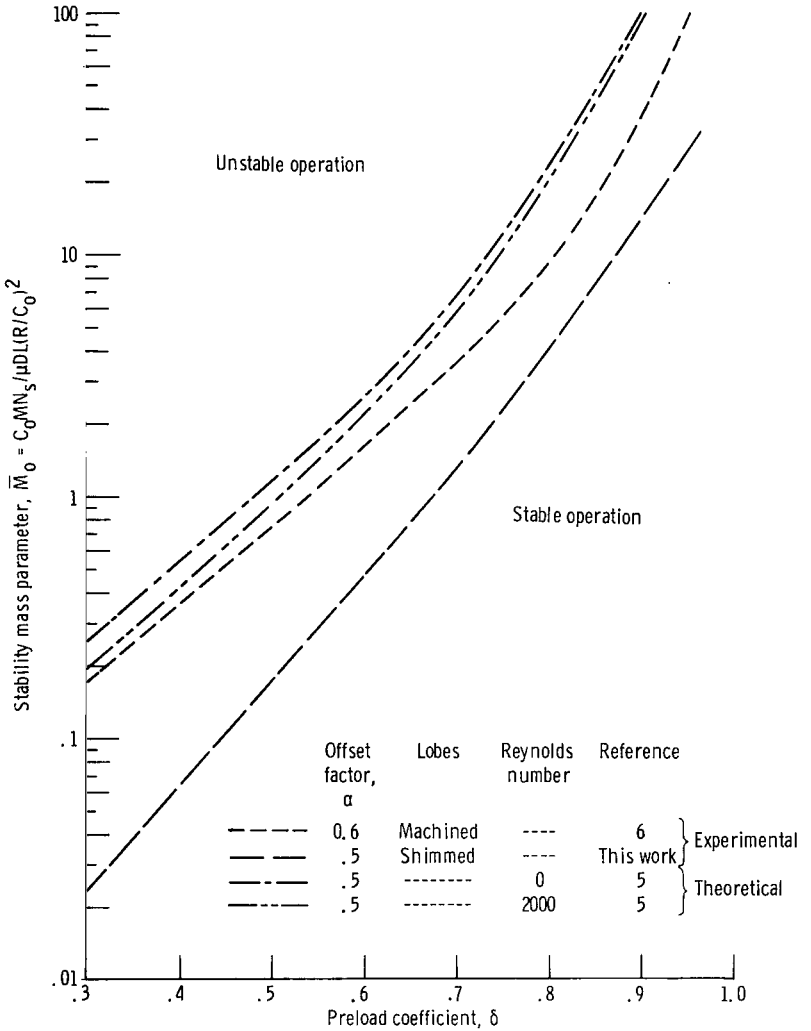

Figure 9. - Comparison of theoretical data for bearings with offset factor of 0.5 and experimental data for bearings with offset factors of 0.5 and 0.6.

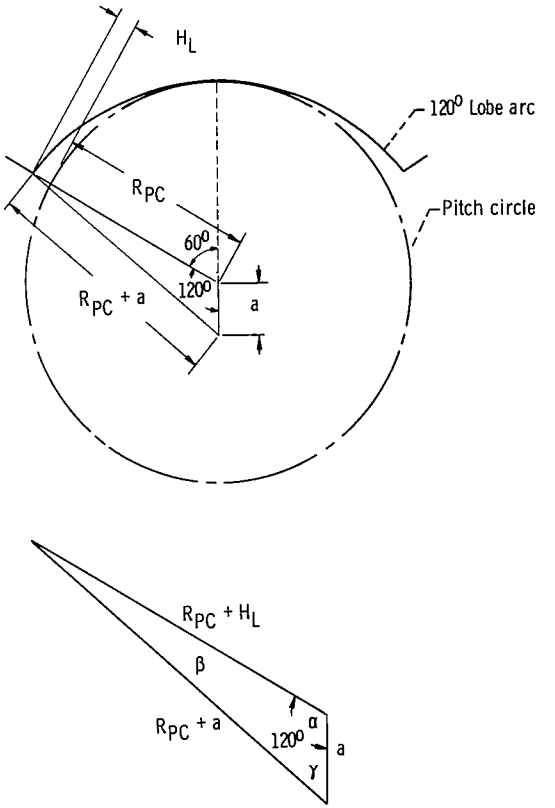

Figure 10. - Method of calculating preload a, lobe radius R_P, and preload coefficient δ, from measured value of lobe height H_L.

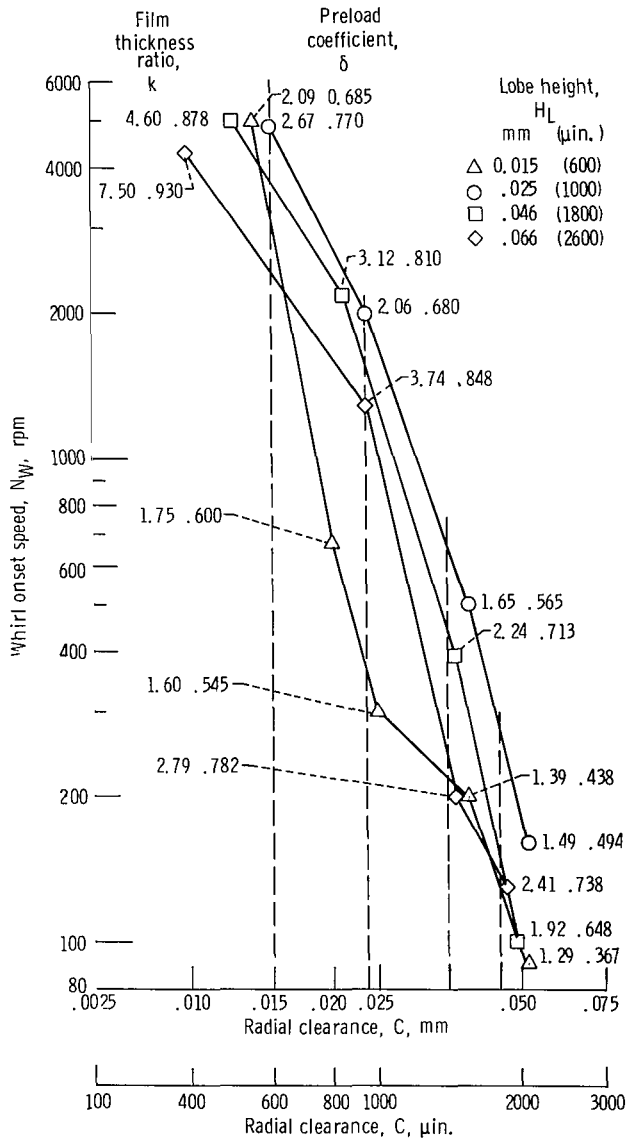

Figure 11. - Whirl onset speed as function of radial clearance at various film thickness ratios and preload coefficients for three-lobe bearing with axial grooves.

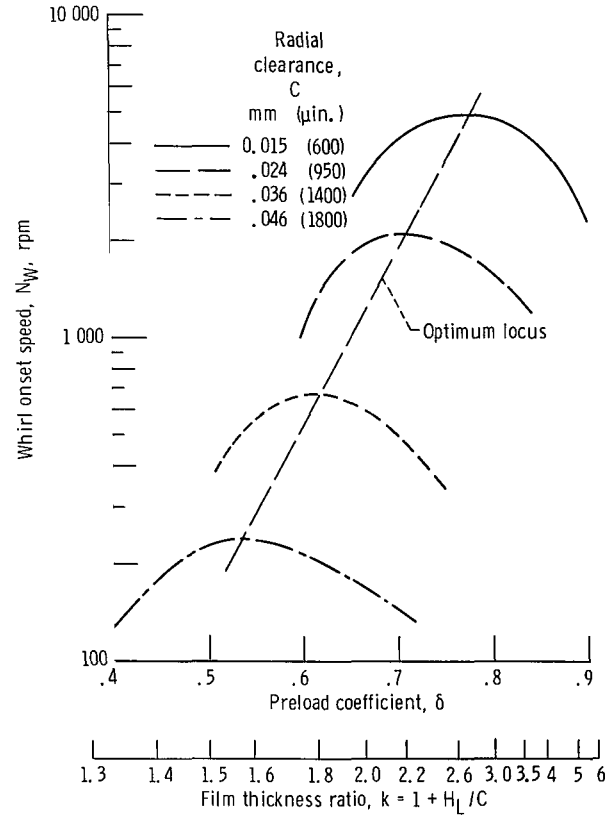

Figure 12. - Whirl onset speed as function of preload coefficient and film thickness ratio for three-lobe bearing with axial grooves.

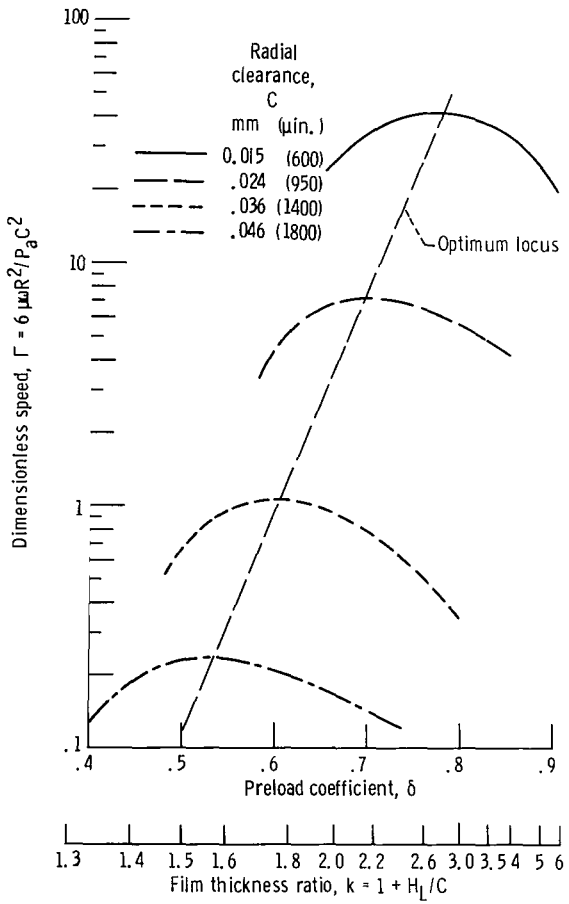

Figure 13. - Dimensionless speed as function of preload coefficient and film thickness ratio for three-lobe bearing with axial grooves.

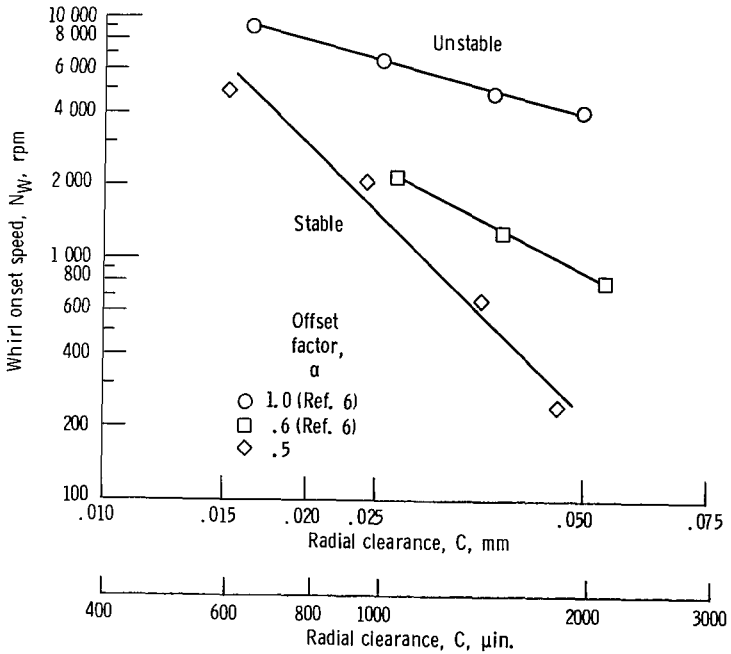

Figure 14. - Comparison of stability of three-lobe bearings at various offset factors.